



# The Pan-STARRS1 view of the Hyades cluster

B. Goldman<sup>1</sup>, S. Röser<sup>2</sup>, E. Schilbach<sup>2</sup>, E. A. Magnier<sup>3</sup>, C. Olczak<sup>2,1,4</sup>,  
T. Henning<sup>1</sup>, and the Pan-STARRS1 Science Consortium

<sup>1</sup> Max Planck Institute for Astronomy, Königstuhl 17, D-69117 Heidelberg, Germany  
e-mail: goldman@mpia.de

<sup>2</sup> Astronomisches Rechen-Institut, Zentrum für Astronomie der Universität Heidelberg,  
Möhhofstrasse 12-14, D-69120 Heidelberg, Germany

<sup>3</sup> Institute for Astronomy, University of Hawaii, Honolulu, HI 96822, U.S.A.

<sup>4</sup> National Astronomical Observatories of China, Chinese Academy of Sciences  
(NAOC/CAS), 20A Datun Lu, Chaoyang District, Beijing 100012, PR China

**Abstract.** The Hyades cluster is an ideal target to study the dynamical evolution of a star cluster over the entire mass range due to its intermediate age and proximity to the Sun. We extend the Hyades mass function towards lower masses down to  $0.1 M_{\odot}$ , and use the full three-dimensional spatial information to characterize the dynamical evolution of the cluster. To this purpose we performed a kinematic and photometric selection using the PPMXL and Pan-STARRS1 sky surveys, to search for cluster members up to 30 pc from the cluster centre. We determined our detection efficiency and field star contamination rate to derive the cluster luminosity and mass functions down to masses of  $0.1 M_{\odot}$ . The thorough astrometric and photometric constraints minimized the contamination. We discovered 43 new Hyades member candidates with velocity perpendicular to the Hyades motion up to  $2 \text{ km s}^{-1}$ . They have mass estimates between  $0.43$  and  $0.09 M_{\odot}$ , for a total mass of  $10 M_{\odot}$ . This doubles the number of Hyades candidates with masses smaller than  $0.15 M_{\odot}$ . We provide an additional list of 11 possible candidates with velocity perpendicular to the Hyades motion up to  $4 \text{ km s}^{-1}$ . We confirm that the cluster is significantly mass segregated but the extension of the mass function towards lower masses provides an even clearer signature than estimated in the past.

**Key words.** Stars: abundances – Open clusters and associations: individual: Hyades – Stars: luminosity function, mass function – Stars: low mass, brown dwarfs

## 1. Introduction

Because of its proximity to the Sun (about 47 pc, for the most recent determinations see, e.g. van Leeuwen 2009; McArthur et al. 2011) and intermediate age (about 650 Myr, see e.g. Perryman et al. 1998; DeGennaro et al. 2009),

the Hyades cluster is a valuable target to study the evolution of stellar clusters.

It is desirable to extend the Hyades census to lower masses to provide new benchmark objects at the end of the main sequence, with known age and metallicity (see the contribution of T. Kopytova in this volume). They can further constrain evolutionary models of the

---

*Send offprint requests to:* B. Goldman

stellar core, of the stellar rotation, and other stellar properties.

The Hyades cluster has a relatively large space velocity of  $(U, V, W) = (-41, -19, -1) \text{ km s}^{-1}$ . This allows us to efficiently remove contaminants based on the proper motion. Röser et al. (2011, R11 thereafter) searched the vicinity of the Hyades cluster up to 30 pc from the centre, using the convergent point method and the wide-area surveys PPMXL (Röser et al. 2010) and CMC14.

The kinematic selection needs to be complemented by a photometric selection in order to improve the purity of the candidate sample. The Panoramic Survey Telescope And Rapid Response System (Pan-STARRS) provides us with the required depth, and large sky multi-band coverage. This data set allows us to push the study of R11 to greater depths and lower masses, and refine the member selection using multi-band photometry and astrometry unavailable until now.

In this presentation, we describe the Pan-STARRS1 observations to date in Sect. 2, the kinematic and photometric selection of the Hyades candidates in Sect. 3, and the resulting present-day mass function in Sect. 4.

## 2. The Pan-STARRS1 project

Pan-STARRS will eventually comprise multiple telescopes and cameras, and currently consists of a single telescope and camera known as Pan-STARRS1 (or PS1; Kaiser et al. 2002). PS1<sup>1</sup> is a new optical/red survey instrument with a large figure of merit thanks to its 7-deg<sup>2</sup> field of view. It uses a dedicated 1.8-m telescope located in Haleakalā on Maui. The pixel scale is 0.25 arcsec pix<sup>-1</sup>. A set of six filters is available: *griz* roughly similar to the SDSS filter system, with some differences such as a red cut-off in the *z* band, a *y* band around 1 μm, and a broad *w* filter roughly covering *g*, *r* and *i* for Solar system observations.

PS1 started regular survey operation in April 2010. The observing time is split between several surveys, the  $3\pi$  survey which

we describe below, for 60% of the useful observing time; the Medium Deep Fields survey, which covers ten fields (over the whole year) in five on a nightly basis, for 23%; and several surveys making a smaller portion of the time, such as a transiting exo-planet search Pan-Planet, a search for asteroids, a monitoring of the Andromeda galaxy

Here we use the data of the  $3\pi$  survey, which covers in the five *grizy* filter all the sky north of  $-30^\circ$ . It performs four visits of each sky location every year, in each filter. About 25% of each exposure footprint is not observed because of the gaps between the sensitive devices and the masked areas due to bright stars, trails, etc. The median image quality ranges from 1''.3 in the *g* band to 1''.0 in the *y* band. The median single exposure 5- $\sigma$  depth is 22.0 mag (AB) in the *g* band, 21.8 mag in the *r* band, 21.5 mag in the *i* band, 20.8 mag in the *z* band. The data are photometrically calibrated according to the algorithm of Schlafly et al. (2012), who use repeated observations of the same stars to constrain a model for the PS1 system throughput. Internal comparisons and comparison with the SDSS indicate that the photometric calibration is accurate at the  $< 1\%$  level.

The images accumulated over the first 18 months have been stacked to produce a deeper, static image of the sky. For instance, the median 10- $\sigma$  depth in the *z* band is 21.2 mag, about 1.3 mag deeper than SDSS.

In the following we use the  $3\pi$  observations of the 10% of the sky centered on the Hyades cluster centre, which we define at RA=4<sup>h</sup> 28<sup>m</sup> 25.7<sup>s</sup>, Dec=+16° 42' 45'' (J2000.0). The survey has accumulated more than two years of survey data, with multiple *grizy* coverage of the Hyades.

We use data obtained until August 2012. Over this observing period, PS1 has incomplete sky coverage of the Hyades, because of adverse weather pattern in the past two winter seasons. However, the fraction of 2MASS stars over the area of interest with good PS1 detections in either of *g*, *r* or *i* band is 94%. These filters offer the largest wavelength span with 2MASS *K<sub>s</sub>* band, and best rejection of

<sup>1</sup> [www.ps1sc.org](http://www.ps1sc.org)

field stars (see next Section), and together an almost complete coverage.

### 3. Candidate selection

The membership selection is a three step process. First, we select kinematic members by the convergent point method. Second, we further restrict the sample of candidates by photometric selection. Finally, we verify the PPMXL proper motions for all the candidates that survived the kinematic and photometric selections.

#### 3.1. Kinematic selection

The convergent point method (CPM; for a detailed recent description, see van Leeuwen 2009) is an important tool to isolate (from the field) an ensemble of stars sharing the same 3D-space motion such as the stars in an open cluster. We follow the approach of R11 (Sect. 4.1) and select only stars within a radius of 30 pc around the centre of the cluster.

For each object with small PPMXL proper motion error ( $< 20 \text{ mas yr}^{-1}$ ) and 2MASS “A” flag in  $J$  and  $K_s$  bands, assuming Hyades membership, the CPM provides an estimate of the secular distance, a prediction of the radial velocity, and the velocity component  $|v_{\perp}|$  perpendicular to the direction to the convergent point. We allow a limit of  $4 \text{ km s}^{-1}$  for this latter parameter, an upper bound to the angle between the proper motion vector and the vector in the direction to the convergent point, of  $9.5^\circ$ , in order to limit the contamination for candidates closer to the convergent point.

In order to increase the purity of our sample, we further require our candidates to have  $|v_{\perp}| < 2 \text{ km s}^{-1}$ . We find that these parameters offer a good compromise of purity and completeness: The stronger constraint roughly decreases by a factor of two the field contamination (based on our Besançon simulation, see Section 4). On the other hand, a residual velocity of  $2 \text{ km s}^{-1}$  is still much larger than the velocity dispersion in the cluster, which is predicted to be smaller than  $1 \text{ km s}^{-1}$  (see R11; Ernst, priv. comm.). However, we note that some binaries may display orbital motion that

modifies the calculation of  $|v_{\perp}|$ . For instance, the bona fide Hyades binary member 77 Tau, with Hipparcos proper motion measurement, has  $|v_{\perp}| = (2.33 \pm 0.05) \text{ km s}^{-1}$ .

We select 16543 kinematic candidates, with partial overlap with the list published in R11.

#### 3.2. Photometric selection

As R11 describe, the CPM is no final confirmation for a star to be co-moving with the bulk of the Hyades cluster, it “predicts” a secular parallax and a radial velocity for each candidate. Both quantities have to be verified to conclusively confirm membership. Using the predicted secular parallaxes one is able to construct colour-absolute magnitude diagrams (depending on the observed bands) to check if the candidates populate allowed loci in these diagrams.

We define our selection box empirically in colour-magnitude diagrams (see Fig. 1), as atmospheric models of the low-mass stars do not reproduce the over-density in the CMD due to the Hyades sequence. We perform this selection using  $g - K$ ,  $r - K$ , and/or  $i - K$  colors, depending on the available data. We note that the discrimination between the Hyades cluster sequence and the bulk of the background stars is the better the larger is the wavelength difference between the bands. When multiple colors are available we require all conditions to be satisfied.

Most of the field stars do not share the cluster motion, so that their kinematic parallax is erroneous and their calculated absolute magnitude does not correspond to that of a Hyades-sequence star of their colour.

We select 273 PS1 candidates objects with  $|v_{\perp}| < 4 \text{ km s}^{-1}$ .

#### 3.3. Final selection

We perform additional selections in order to check the PPMXL proper motions of the candidates, as large PPMXL proper motions are known to be often erroneous due to mismatches in USNO-B1.0. We use PS1 astrom-

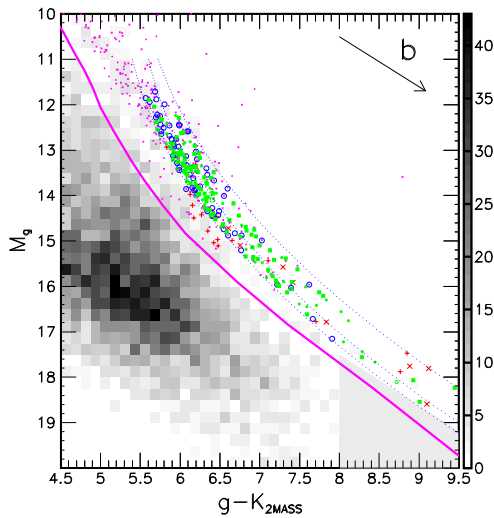


**Fig. 1.** Hess diagrams of  $g_{P1} - K_{2MASS}$  for the all kinematic candidates, i.e. with  $|v_{\perp}| < 4 \text{ km s}^{-1}$  up to 30 pc from the cluster centre. Filled [green] circles indicate candidates selected in  $g$ ,  $r$  and  $i$ ; open [blue] circles: candidates selected in one or two filters; [red] crosses and pluses: candidates suspected to be giants, or to have bad proper motion measurements. Dots [magenta] represent R11 Hyades candidates. The dotted [blue] lines indicate our selection zone, while the thick [magenta] line represents the BT-Settl model 600-Myr isochrone. The grey area at the faint, red edge shows our incompleteness limit.

etry, as well as near-IR colour-colour diagram and WISE data to remove candidates with poor measurements, or suspected to be background giants. We combine our sample with the candidates of R11 which are saturated in the PS1 data and cannot be confirmed by our analysis. Our analysis returns 54 new Hyades candidates, mostly at the low-mass end of the main sequence.

#### 4. Hyades mass function

We perform a detailed analysis of the sensitivity of our data, in order to determine our detection efficiency. We find that PPMXL limits our sensitivity with a detection efficiency of a  $0.1 M_{\odot}$  star at a distance of 77 pc (30 pc beyond the cluster centre) of about 50%.

We also perform a full simulation of our observations for a catalogue of “mock” stars

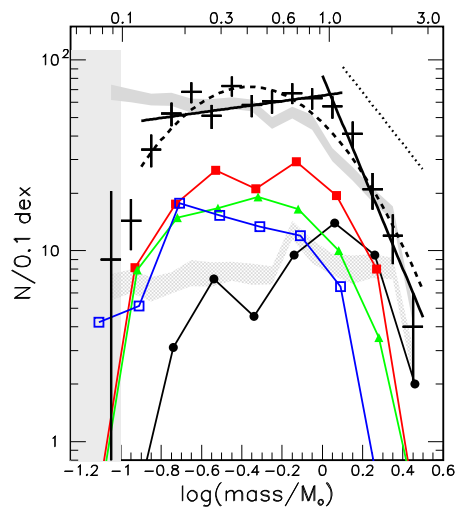


**Fig. 2.** Corrected mass function (number of candidates with  $|v_{\perp}| < 2 \text{ km s}^{-1}$ ) of the Hyades in the 2MASS  $K_s$  band, for regions of various cluster radii: 0 to 3.1 pc (circle); 3.1 to 9 pc (filled square); 9 to 18 pc (triangle); and 18 to 30 pc (open square). The top histogram shows the complete mass function up to 30 pc, fitted with two power laws (thick lines), and a log-normal mass function (dashed line). The Salpeter mass function is shown for comparison (dotted line). The grey areas are the  $1\text{-}\sigma$  locus of the simulation of Ernst et al. (2011) for the cluster centre ( $r_c < 3 \text{ pc}$ , bottom) and the whole volume ( $r_c < 30 \text{ pc}$ , top). The light grey area for  $m < 0.1 M_{\odot}$  indicates the masses for which our results are strongly affected by incompleteness.

with kinematics and Johnson-Cousins  $BVRIC$  photometry as predicted by a Besançon model realization of the Galaxy (Robin et al. 2003). We subtract this contamination estimate from the density of our candidates.

Finally, we transform the luminosity of the new candidates using the mass-luminosity relation provided by Baraffe et al. (1998), used in the  $K_s$  band, as the models prove to better match the observations for that filter (R11, see Fig. 2). We find that the mass function in the range of  $0.13\text{--}3.2 M_{\odot}$  is well fitted with a log-normal function (Chabrier 2003),  $\xi(m) = e^{-(\log m - \log m_c)^2 / 2\sigma^2}$ , with parameters:  $m_c = (0.44 \pm 0.03) M_{\odot}$  and  $\sigma = 0.39 \pm 0.02$ .

## 5. Conclusions

We have combined the PPMXL and Pan-STARRS1 catalogues to search for low-mass Hyades members up to 30 pc from the cluster centre. We select candidates based on the PPMXL kinematics and Pan-STARRS1 astrometry and photometry, combined with 2MASS, WISE and SDSS photometry, to produce a clean sample of candidates nearly complete down to  $0.1 M_{\odot}$ .

We discover 54 new candidates, with an average mass of  $0.18 M_{\odot}$  and an average distance from the cluster centre of 18 pc. We select a purer sample of 43 new candidates with velocity perpendicular to the Hyades motion smaller than  $2 \text{ km s}^{-1}$ . This doubles the number of Hyades candidates for masses smaller than  $0.15 M_{\odot}$ .

We find that the mass function is nearly flat for masses between  $0.1$  and  $1 M_{\odot}$ , with  $-\alpha = 0.15 \pm 0.06$ . Using the minimum spanning tree measure  $\Gamma_{\text{MST}}$  (Olczak et al. 2011) we find the cluster is clearly segregated in mass, with the lowest-mass members having been removed from the cluster centre to the outer region.

The Hyades cluster is close enough that PS1 will eventually measure the parallaxes of all low-mass star and L-type-dwarf cluster candidates within 30 pc of the centre. This will provide a strong confirmation for memberships, and allow a detailed analysis of the kinematics, binarity, activity of the cluster members. In the pre-Gaia area, the Hyades will

therefore be a unique test of cluster evolution and of pre-main sequence evolution of low-mass stars.

*Acknowledgements.* We thank Steve Boudreault, Andreas Ernst and France Allard for providing material from their publications, as well as Mario Gennaro and Josh Schlieder for their comments. This work was supported by Sonderforschungsbereich SFB 881 “The Milky Way System” (subproject B6) of the German Research Foundation (DFG). C.O. appreciates funding by the German Research Foundation (DFG) grant OL 350/1-1, support by NAOC CAS through the Silk Road Project, and by Global Networks and Mobility Program of the University of Heidelberg (ZUK 49/1 TP14.8 Spurzem).

## References

- Baraffe, I., et al. 1998, *A&A*, 337, 403
- Chabrier, G. 2003, *PASP*, 115, 763
- DeGennaro, S., et al. 2009, *ApJ*, 696, 12
- Ernst, A., et al. 2011, *A&A*, 536, A64
- Kaiser N., et al. 2002, in *SPIE Conference Series*, Vol. 4836, eds. J. A. Tyson & S. Wolff, 154
- McArthur, B. E., et al. 2011, *AJ*, 141, 172
- Olczak, C., Spurzem, R., & Henning, T. 2011, *A&A*, 532, 119
- Perryman, M. A. C., et al. 1998, *A&A*, 331, 81
- Robin, A. C., et al. 2003, *A&A*, 409, 523
- Röser, S., et al. 2010, *AJ*, 139, 2440
- Röser, S., et al. 2011, *A&A*, 531, 92 (R11)
- Schlafly, E., et al. 2012, *ApJ*, 756, 158
- van Leeuwen, F. 2009, *A&A*, 497, 209